Recombination R-triplex: H-bonds contribution to stability as revealed with minor base substitutions for adenine

Anna K. Shchyolkina, Dmitry N. Kaluzhny, Donna J. Arndt-Jovin[1], Thomas M. Jovin[1] and Victor B. Zhurkin[2,*]

Engelhardt Institute of Molecular Biology, Russian Academy of Sciences, 119991 Moscow, Russia, [1]Department of Molecular Biology, Max Planck Institute for Biophysical Chemistry, D-37070 Goettingen, Germany and [2]Laboratory of Cell Biology, National Cancer Institute, NIH, Bethesda, MD 20892, USA

ABSTRACT

Several cellular processes involve alignment of three nucleic acids strands, in which the third strand (DNA or RNA) is identical and in a parallel orientation to one of the DNA duplex strands. Earlier, using 2-aminopurine as a fluorescent reporter base, we demonstrated that a self-folding oligonucleotide forms a recombination-like structure consistent with the R-triplex. Here, we extended this approach, placing the reporter 2-aminopurine either in the 5′- or 3′-strand. We obtained direct evidence that the 3′-strand forms a stable duplex with the complementary central strand, while the 5′-strand participates in non-Watson–Crick interactions. Substituting 2,6-diaminopurine or 7-deazaadenine for adenine, we tested and confirmed the proposed hydrogen bonding scheme of the A∗(T·A) R-type triplet. The adenine substitutions expected to provide additional H-bonds led to triplex structures with increased stability, whereas the substitutions consistent with a decrease in the number of H-bonds destabilized the triplex. The triplex formation enthalpies and free energies exhibited linear dependences on the number of H-bonds predicted from the A∗(T·A) triplet scheme. The enthalpy of the 10 nt long intramolecular triplex of $-100\ \mathrm{kJ \cdot mol^{-1}}$ demonstrates that the R-triplex is relatively unstable and thus an ideal candidate for a transient intermediate in homologous recombination, t-loop formation at the mammalian telomere ends, and short RNA invasion into a duplex. On the other hand, the impact of a single H-bond, $18\ \mathrm{kJ \cdot mol^{-1}}$, is high compared with the overall triplex formation enthalpy. The observed energy advantage of a 'correct' base in the third strand opposite the Watson–Crick base pair may be a powerful mechanism for securing selectivity of recognition between the single strand and the duplex.

INTRODUCTION

The alignment of three strands of nucleic acids, in which the third strand is identical and oriented parallel to one of the DNA duplex strands, occurs in recombination (1), at telomeres during t-loop formation (2), in DNA rearrangements caused by replication of mitochondrial DNA (3), and has been invoked in initiation of heterochromatin by small hairpin RNAs (4). In principle, such an alignment is capable of forming the R-triplex structure (recombination triplex DNA) as well as a strand exchange structure (D-loop) resulting from the third strand invasion into the duplex. An R-triplex (or R-form DNA) structure was predicted theoretically (5) to consist of isomorphic R-triplets; i.e. the putative R-triplex can accommodate any arbitrary sequence. R-type hydrogen bond schemes for the G∗(C·G) and C∗(G·C) triplets have been visualized by X-ray analysis (6,7), while the T∗(A·T) and A∗(T·A) triplets were verified by FTIR (8,9). Data supporting the existence of the R-triplex in protein-free systems derived from UV and fluorescence thermal denaturation curves, chemical probing, as well as gel shift and FRET assays (10–13) have been published by our laboratories.

Special oligonucleotide constructs (RCW fold) consisting of three strands connected with nucleotide linkers (Figure 1) in which the 5′-terminal strand is denoted as R (Recombination), the central strand as C (Crick, 'complementary') and the 3′-strand as W (Watson) have been used to study the alignment of the strands (13). The two linker loops differ in their conformational flexibility, the GAA loop being extremely stable, while the TTTT loop is less rigid. Importantly, such an RCW fold can accommodate any nucleotide sequence with the two identical R- and W-strands and a complementary C-strand.

*To whom correspondence should be addressed. Tel: +1 301 496 8913; Fax: +1 301 402 4724; Email: zhurkin@nih.gov
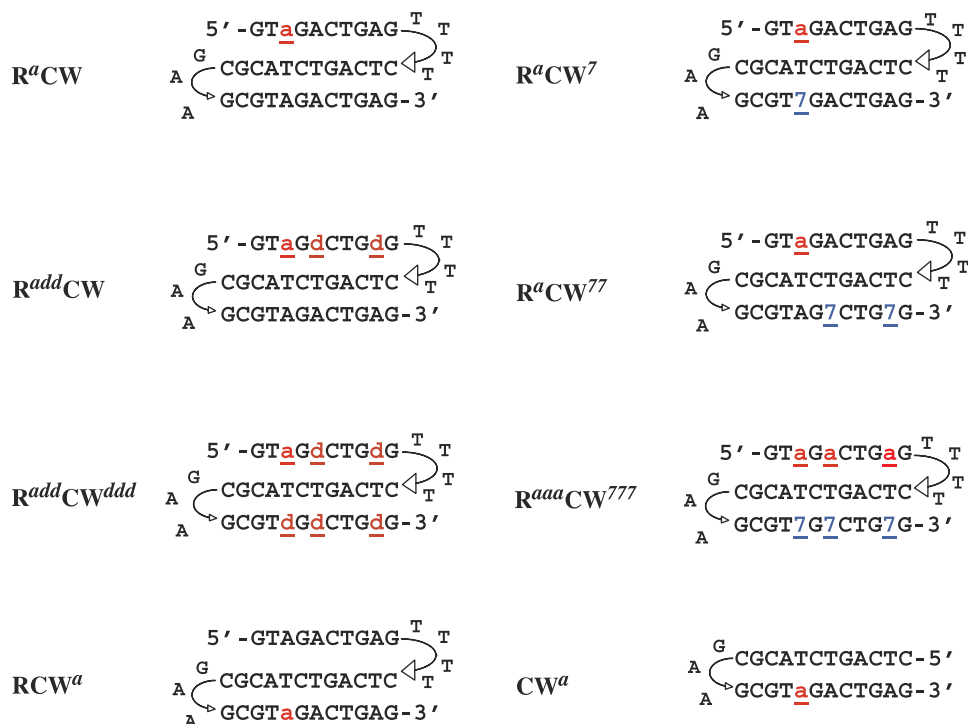
Figure 1. Oligonucleotide sequences with the reporting 2AP base, used in the experiments. *a*, 2-aminopurine (2AP); *d*, 2,6-diaminopurine (DAP); *7*, 7-deazaadenine (7DAA). The triplex-forming oligonucleotides: R^aCW [denoted earlier (13) as $R^{2AP}CW$] contains 2AP in the third R-strand; RCW^a contains 2AP in the W-strand; $R^{add}CW$ has two adenines in the third R-strand substituted for DAP; $R^{add}CW^{ddd}$ has the two adenines in the R-strand and the three adenines in the W-strand substituted for DAP; R^aCW^7 contains a 2AP∗(T·7DAA) triplet with 2AP in the R-strand and 7DAA in place of the adenine in W-strand; R^aCW^{77} contains two A∗(T·7DAA) triplets; $R^{aaa}CW^{777}$ is the triplex with three 2AP∗(T·7DAA) triplets. The hairpin-forming oligonucleotide, CW^a, represents the duplex part of the triplex RCW^a.
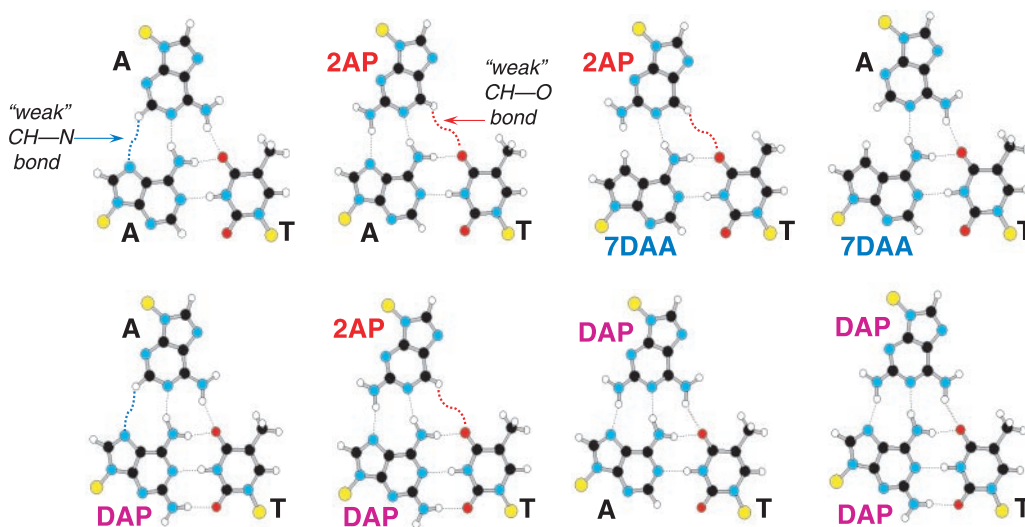

Figure 2. Schematic representation of the isogeometric base triplets accommodating 2-aminopurine (2AP), 2,6-diaminopurine (DAP) and 7-deazaadenine (7DAA).

We demonstrated previously that the fluorescent base analog, 2-aminopurine (2AP), can be substituted for adenine in the A∗(T·A) triplet, forming the 2AP∗(T·A) triplet, stereochemically consistent with the R-form (Figure 2). The temperature-dependent cooperative dissociation of the R-strand from the duplex was detected by two techniques: (i) fluorescence of the 2AP which monitored disruption of the individual A∗(T·A) triplet and (ii) conventional UV absorbance at 260 nm reflecting melting of the third strand as a whole. Both methods revealed the same temperature-dependent cooperative dissociation of the R-strand from the duplex part (13), thus demonstrating that the fluorescence of the 2AP reported faithfully the thermodynamic parameters of the RCW triplex fold.

In the present work, we extended this approach by placing the fluorescent 2AP and other substitutions for adenine, site-specifically, either in the 5′- or 3′-strand. These substitutions allowed us (i) to monitor the difference in conformational behavior between the two identical R- and W-strands in the RCW fold and (ii) to obtain quantitative data on the energetics of the R-triplex formation. In particular, we were interested in deducing the relative impact of the base–base interactions in the duplex part of the triplex, and between the duplex and the third strand, i.e. issues directly related to the fidelity of nucleic acid recognition.

MATERIALS AND METHODS

Oligonucleotides

R^aCW, RCW^a, $R^{add}CW$, R^aCW^7, R^aCW^{77}, $R^{aaa}CW^{777}$ and CW^a were synthesized and purified by high-performance liquid chromatography by Midland Certified Reagent Co. Inc. (TX); $R^{add}CW^{ddd}$ and RCW^a were synthesized and purified in PAAG by Syntol (Moscow) (for designations and folding schemes see Figure 1). The hydrogen bonding schemes for the A∗(T·A) triplet and the triplets with 2AP, 2,6-diaminopurine (DAP) and 7-deazaadenine (7DAA) substitutions tested in the study are given in Figure 2. Samples contained 0.9–1.4 µM oligonucleotides, 0.5 M LiCl and 10 mM Tris–HCl buffer, pH 7.6.

Fluorescence measurements

The temperature dependence of the fluorescence emission of oligonucleotides containing a single 2AP substitution were recorded with a Cary Eclipse fluorescence spectrophotometer (Varian) in a thermostated cuvette at the constant heating of 0.5°C/min. The excitation wavelength was 310 nm, and the maximum of the emission was 370 nm. Samples contained 1 µM oligonucleotides, 0.5 M LiCl and 10 mM Tris–HCl buffer, pH 7.6.

UV thermal denaturation profiles

UV thermal denaturation curves were recorded at 260 nm with a Cary 100 Scan UV-visible spectrophotometer (Varian) with a constant heating gradient of 0.5 or 0.2°C/min.

Thermodynamic analysis of the intramolecular triplex formation

The detailed analysis of the thermal denaturation profiles, recorded by fluorescence of the 2AP reporter, has been described elsewhere (13). In essence, we analyzed the intramolecular binding of the dangling third strand to its double-helical CW part by fitting a theoretical curve to the experimental fluorescence melting curve. From these data we deduced the basic thermodynamic parameters of the intramolecular transition (denoted below as the 'triple helix formation').

RESULTS AND DISCUSSION

Probing conformation of the two homologous strands with 2AP

Substitution of 2AP for adenine constitutes an ideal structural probe for testing the RCW fold; the probe neither destabilizes nor distorts the 3D structure (13). Using 2AP as a reporter base in the 5′-strand, we demonstrated previously (13) that the R^aCW oligonucleotide forms a sequence-specific structure, whose conformational equilibrium is shifted toward the R-type triplex. However, in these studies, we presented no direct evidence regarding conformation of the 3′-strand.

To detect the difference in conformation between the two identical R- and W-strands in the RCW fold, we substituted 2AP for adenine in the Watson 3′-strand (Figure 1, RCW^a oligonucleotide) and compared the temperature dependence of the fluorescence intensity for RCW^a with those for CW^a and R^aCW (Figure 3A). The enhancement of R^aCW fluorescence (circles) in the temperature range from 5 to 40°C
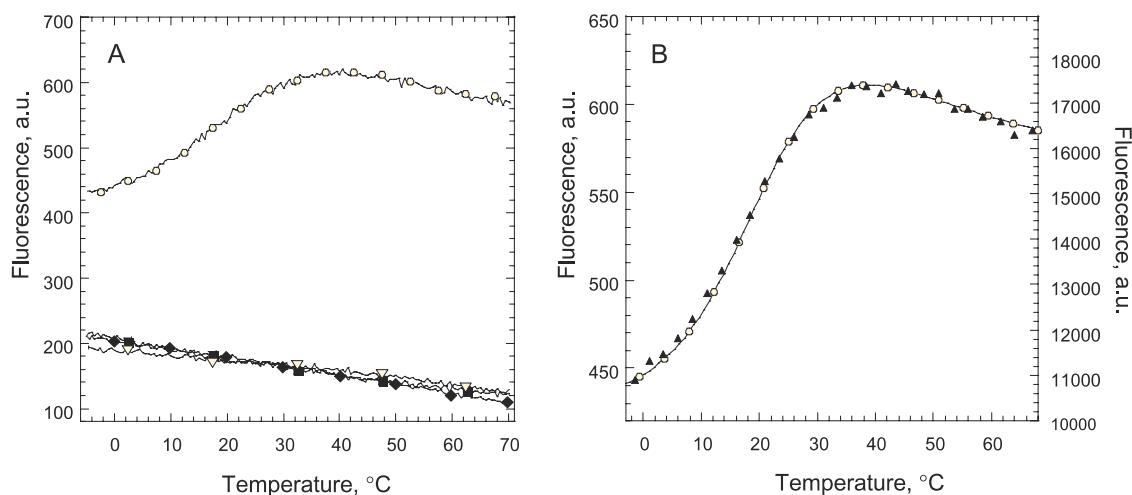

Figure 3. (**A**) Temperature dependence of the fluorescence emission of 2AP, incorporated in the oligonucleotides: R^aCW (open circles), RCW^a (squares), CW^{2AP} (diamonds) and $R^{add}CW$ (open triangles). Every 10th experimental point is marked. The excitation wavelength was 310 nm, emission was measured at 370 nm. Samples contained 1 µM oligonucleotides, 0.5 M LiCl and 10 mM Tris–HCl buffer, pH 7.6. *Note*: comparison between 2AP in the duplex and in the third strand of the triplex. (**B**) Temperature dependence of the fluorescence emission of 2AP incorporated in the R^aCW at different concentrations of the oligonucleotide: 1 µM (open circles), 50 µM (filled triangles). The fluorescence was measured in 3 and 1.5 mm cells, respectively.

reflected increasing exposure of 2AP to solvent due to melting of the triplex, namely a progressive loss of the 2AP stacking with the adjacent bases. Above 35–40°C, the R^aCW melting profile followed that of the single R2AP strand (13). The temperature profile for the RCW^a oligonucleotide was entirely different. In this case, the fluorescence monotonically decreased (Figure 3A, squares), similar to the profile for the double-stranded hairpin CW^a (Figure 3A, diamonds). These results, and the fact that the RCW^a and CW^a oligonucleotides fluoresce similarly at equal concentrations, demonstrated that the fluorophore is in the same state in the RCW^a and CW^a folds, showing a temperature dependence of 2AP fluorescence that is typical for a DNA duplex. Thus, we conclude that the Watson 3′-strand retains base pairing with the complementary Crick strand under our experimental conditions.

The specific features of the melting profiles of 2AP fluorescence are likely related to a relatively hydrophobic environment with considerable base stacking inside the double helix (14) resulting in a markedly quenched fluorescence of the 2AP compared with that of 2AP in the third strand of the triplex. Further quenching of fluorescence of 2AP located within the double helix was probably promoted with increasing temperature through the non-radiative relaxation of excited states (15). A dynamic invasion of the 5′-strand in the Watson–Crick duplex displacing the identical 3′-strand appears improbable, as it would have caused a detectable increase in the 2AP fluorescence in RCW^a compared with CW^a. In other words, these data provide direct evidence against a dynamic mixture of two different duplex folds, i.e. branch migration structure, whereby the complementary C-strand is partially paired with both the 5′- and the 3′-strand.

Interpretation of the data is based on the assumption that the oligonucleotides form intramolecular folds rather than intermolecular associates. The nucleotide sequence, salt conditions and the procedure for the sample preparation have been selected to avoid formation of intermolecular species (13). The intramolecular character of the R^aCW folding has been demonstrated by evaluating the oligonucleotide hydrodynamic volume under these experimental conditions (13). Here, we present additional, independent evidence for the intramolecular folding of R^aCW by comparing melting curves for two concentrations of the oligonucleotide at 1 and 50 μM (Figure 3B). The identity of two melting transitions for the concentrations differing by 50-fold unambiguously corroborates the intramolecular folding of the R^aCW oligonucleotide.

2,6-Diaminopurine substitutions for adenines in the homologous R- and W-strands

To gain further information about the RCW fold structure, we made substitutions of adenines by DAP in the Watson and/or R-strands. The oligonucleotide $R^{add}CW$ contained two diaminopurines in the R-strand (Figure 1) in addition to the 2AP as in R^aCW. Potentially, these additional substitutions would lead to formation of two DAP∗(T·A) triplets (Figure 2), thereby stabilizing the RCW triplex through the additional H-bond in these triplets. Alternatively, the complementary C-strand may 'change' partners and form a canonical duplex with the 5′-R-strand (strand invasion), since DAP is

known to pair with thymine forming three hydrogen bonds (16). We measured the temperature-dependent 2AP fluorescence of $R^{add}CW$ to distinguish between these two possibilities.

The temperature-dependent fluorescence curve of the $R^{add}CW$ oligonucleotide (Figure 3A, triangles) gave a similar profile to that of CW^a (Figure 3A, diamonds) and RCW^a (Figure 3A, squares), but different from that of R^aCW (Figure 3A, circles). Based on these data, we conclude that the 5′-strand forms a duplex with the C-strand, which involves two stable T·DAP base pairs. Therefore, introduction of two DAP molecules in the 5′-strand strongly affects the mode of RCW folding and promotes strand exchange as opposed to an R-triplex. Note that the rearrangement of the RCW fold observed here upon the A substitutions by DAP in the R-strand is topologically equivalent to the strand exchange promoted by RecA protein (1,5).

In oligonucleotide $R^{add}CW^{ddd}$, DAP was substituted for the adenines in both the 5′-R- and 3′-W-strands except for the reporter 2AP in the R-strand (Figure 1). According to the triplet scheme of Figure 2, we expected the two DAP∗(T·DAP) triplets to stabilize the RCW fold by providing additional hydrogen bonds. Indeed, the $R^{add}CW^{ddd}$ construct has a higher stability as follows from the fact that the temperature-dependent fluorescence profile is shifted rightward (Figure 4, circles).

Although DAP absorbs weakly at 310 nm, it was necessary to assess the potential contribution of the five DAP residues in the $R^{add}CW^{ddd}$ construct to the $R^{add}CW^{ddd}$ emission upon excitation at this wavelength. We compared the $R^{add}CW^{ddd}$ fluorescence melting curve with the transition registered by UV absorption at 260 nm (Figure 4, inset,
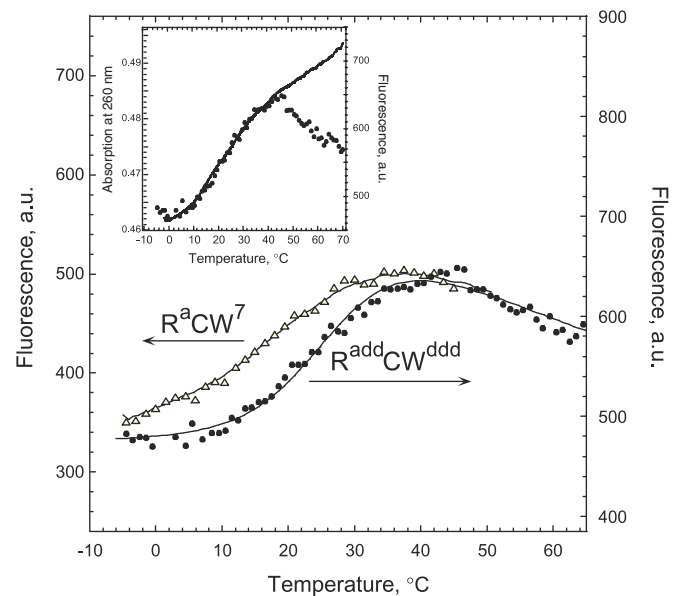

Figure 4. Temperature dependence of the fluorescence emission of 2AP incorporated in the oligonucleotides: R^aCW^7 (open triangles), left ordinate; $R^{add}CW^{ddd}$ (circles), right ordinate. Solid curves are the best theoretical fits [Materials and Methods and Ref. (13)]. Derived thermodynamic parameters are given in Table 1. The experimental conditions are the same as in Figure 3. Inset: comparison of the $R^{add}CW^{ddd}$ melting curves registered with fluorescence (circles, right ordinate) and with absorption at 260 nm (solid curve, left ordinate).

Table 1. Thermodynamic parameters of the R-triplex formation

Oligonucleotide	ΔH (kJ·mol^{-1})	ΔS (kJ·mol^{-1}·deg^{-1})	T_m (°C)	$\Delta G(0°C)$ (kJ·mol^{-1})	Δ(Number of H-bonds) compared with R^{a}CW [a]
R^{add}CW^{ddd} [b]	-126 ± 7	-0.420 ± 0.005	27 ± 1	-11.3 ± 0.7	+2
R^{a}CW [b]	-99 ± 3	-0.337 ± 0.005	21 ± 1	-7.1 ± 0.5	0
R^{a}CW^7 [b]	-84 ± 3	-0.289 ± 0.007	20 ± 1	-5.2 ± 0.7	-1
R^{a}CW^{77} [b,c]	-74 ± 2	-0.254 ± 0.005	18 ± 1	-4.6 ± 0.7	-2 ('weak' H bonds)
R^{aaa}CW^{777} [d]	-45 ± 3	-0.153 ± 0.005	15 ± 1	-2.3 ± 0.7	-3

[a]Predicted Δ(Number of H-bonds) between the R-strand and the CW duplex compared with that in R^{a}CW, according to the R-triplex model (5).
[b]Thermodynamic parameters obtained from the fluorescence emission melting curves.
[c]The R^{a}CW^{77} fold has two A∗(T·7DAA) triplets (Figure 2) which are less stable than the 'standard' 2AP∗(T·A) triplets, because the former are unable to form 'weak' CH···N hydrogen bonds (5,19).
[d]Thermodynamic parameters obtained from the UV absorption melting curves.

circles and solid line, respectively). The two curves coincide below 40°C, i.e. in the region where the UV melting reflects mainly the thermal dissociation of the third stand from the more stable duplex part of the R^{add}CW^{ddd}. We conclude that the contribution of DAP fluorescence to the melting profiles of the oligonucleotide R^{add}CW^{ddd} (as well as R^{add}CW, also containing the DAP bases) upon excitation at 310 nm is negligible.

Thermodynamic parameters for this construct as well as for R^{a}CW, determined with our fitting procedure are listed in Table 1. The R^{add}CW^{ddd} triplex melting temperature increased by 6°C, resulting in gain in ΔH of ∼27 kJ·mol^{-1} and an increase in ΔG of ∼4 kJ·mol^{-1} at 0°C (Table 1). Thus, the R^{add}CW^{ddd} construct has the highest stability among the R-triplexes of mixed nucleotide sequences studied so far (10,11,13,17). The increased stability of the DAP∗(T·DAP) triplets compared with the A∗(T·A) triplets is consistent with the proposed H-bonding scheme for the R-triplet (5) (Figure 2).

Testing the H-bonding scheme of the A∗(T·A) triplet with 7-deazaadenine substitutions

To further test the impact of hydrogen bonds on the stability of the R-triplex, we constructed oligonucleotides R^{a}CW^7, R^{a}CW^{77} and R^{aaa}CW^{777} with the 7-deazaadenine (7DAA) substituted for adenine in the Watson strand (Figure 1). In contrast to DAP, the 7DAA substitutions are expected to destabilize the RCW triplex (18). The 7DAA has a CH group in the ring position 7 instead of the negatively charged nitrogen N7. Hence, 7DAA cannot be an acceptor of a proton from the 2AP amino group and instead, the CH group would produce a steric clash with the amino group, thereby destabilizing the 2AP∗(T·7DAA) triplet shown in Figure 2. Similarly, if an adenine is positioned in the 5′-R-strand opposite to 7DAA (see R^{a}CW^{77} in Figure 1), then the A–7DAA interaction is also expected to be unfavorable. In this case, the CH···HC electrostatic interaction (18) would be a major repulsion factor (Figure 2).

Thermal denaturation data for the R^{a}CW^7 triplex are shown in Figure 4 (triangles). R^{a}CW^7 melted earlier than the R^{add}CW^{ddd} triplex by 7°C. Furthermore, the slopes of the melting curves were visibly different, corresponding to a significantly lower formation enthalpy and free energy for the R^{a}CW^7 triplex (Table 1). Comparison of the thermodynamic parameters for the R^{a}CW^7 triplex and the 'reference' R^{a}CW fold indicates that the R^{a}CW^7 is demonstrably less stable than the R^{a}CW (Table 1), although the former differs from the latter by only one hydrogen bond (Figures 1 and 2).

The A∗(T·A) triplet (Figure 2) is presumed to form a 'weak' CH···N hydrogen bond [reviewed in (19)]. To test the contribution of such a bond on R-triplex stability we constructed the oligonucleotide R^{a}CW^{77}, containing two putative A∗(T·7DAA) triplets in addition to a 'standard' reporting 2AP∗(T·A) triplet (Figure 1). This fold lacks two CH···N hydrogen bonds compared to the reference fold R^{a}CW. The impact of this substitution resulted in a decrease in the T_m by 3°C with an associated $\Delta\Delta H = 12 \pm 2$ kJ·mol^{-1} and $\Delta\Delta G(0°C) = 1.2 \pm 0.5$ kJ·mol^{-1} (Table 1 and Supplementary Figure S1). Thus, the 'weak' CH···N hydrogen bond contributes noticeably to the R-triplex stability.

The oligonucleotide R^{aaa}CW^{777} contains three 2AP∗(T·7DAA) triplets, and therefore is expected to lose three hydrogen bonds compared to R^{a}CW (Figures 1 and 2). Fluorescence is not a method of choice for detection of the denaturation profile of R^{aaa}CW^{777} since the 2AP fluorescence emission would be affected by energy transfer between the three closely positioned 2-aminopurines. For this reason, the thermal denaturation profile of R^{aaa}CW^{777} was determined by the UV absorption at 260 nm (Supplementary Figure S2; the derived thermodynamic parameters are presented in Table 1). As expected, the stability of the R^{aaa}CW^{777} triplex was exceptionally low, showing a T_m 6°C lower than that of R^{a}CW with lowered transition enthalpy, entropy and free energy values.

Additive effect of the hydrogen bonds on the R-triplex stability

A graphical representation (Figure 5) of the thermodynamic data (Table 1) accentuates the energy impact of hydrogen bonds on the R-triplex stability. Both the formation ΔHs and ΔGs plotted against the predicted number of hydrogen bonds in the R-triplex (relative to the R^{a}CW fold) may be fitted with straight lines within the limits of experimental errors. Such a linear dependence implies that the global triplex conformation at low temperature is similar for all of the oligonucleotides; i.e. in the simplest case, the overall stability of the intramolecular DNA fold would be proportional to the number of stabilizing hydrogen bonds, as has been postulated previously for double- and H-form triple-stranded DNA structures (20,21).
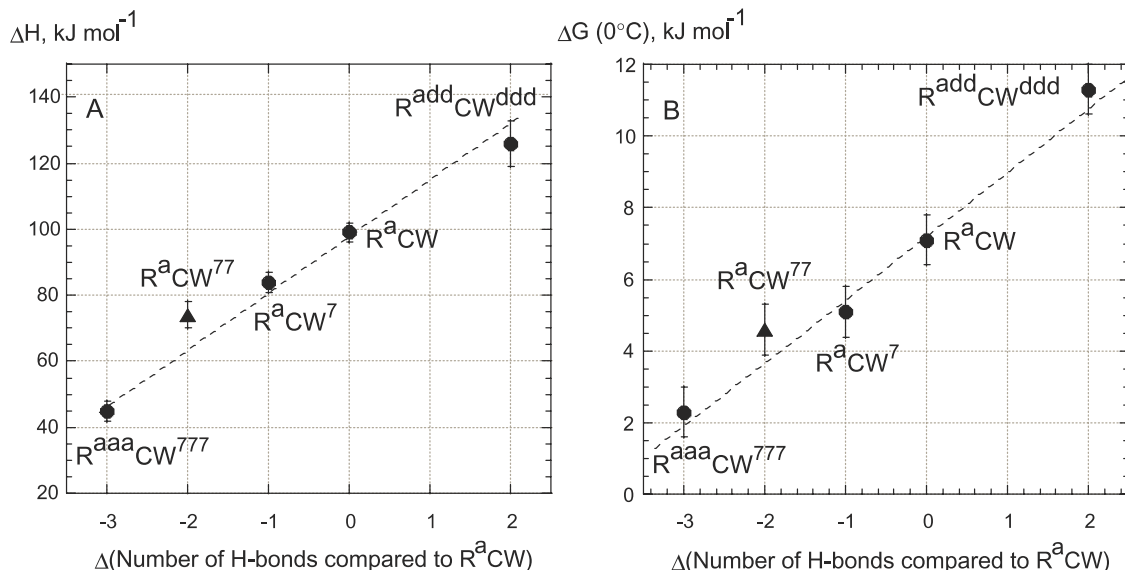
Figure 5. Thermodynamic parameters of the R-triplex formation as functions of the number of predicted hydrogen bonds (compared to R^aCW). (**A**) The absolute values of the formation enthalpy; (**B**) the absolute values of the formation free energy calculated for $0°C$ (Table 1). The triplex folds differ from the R^aCW either by the number of 'standard' $NH\cdots N$ hydrogen bonds (circles), or by the number of the 'weak' $CH\cdots N$ bonds (triangles) (for details see Table 1 and main text). Note that all the circles deviate from the straight fitting lines by less than the limits of experimental errors. The only exceptions are the R^aCW^{77} points lying above these lines and having the enthalpy and free energy values relatively close to the R^aCW values. This is consistent with the $CH\cdots N$ bonds being weaker than the $NH\cdots N$ bonds (5,19).

One may deduce the contribution of a single H-bond in the R-triplex from these data. A mismatch that removes a single H-bond from the triplex reduces the formation enthalpy by $\Delta\Delta H = 18 \pm 1.0 \text{ kJ}\cdot\text{mol}^{-1}$ and the formation free energy by $\Delta\Delta G(0°C) = 1.8 \pm 0.2 \text{ kJ}\cdot\text{mol}^{-1}$ (Figure 5). As a result, the loss of only three H-bonds in the $R^{aaa}CW^{777}$ dramatically destabilizes the triplex and leads to a drop in the absolute value of formation enthalpy from 99 ± 3 to $45 \pm 3 \text{ kJ}\cdot\text{mol}^{-1}$ (54%) and the free energy from 7.1 ± 0.5 to $2.3 \pm 0.7 \text{ kJ}\cdot\text{mol}^{-1}$ (67%). The plots presented in Figure 5 predict that mismatches removing 4–5 hydrogen bonds (two 'wrong' bases) from a potential 10 nt long R-triplex would practically abolish triplex formation under our experimental conditions and prevent recognition of the duplex by the third strand. For various DNA duplexes, the absolute values of $\Delta\Delta G(0°C)$ per H-bond estimated from the data given in Ref. (20) vary from 2 to 10 $\text{kJ}\cdot\text{mol}^{-1}$. An additional hydrogen bond in the $C^+*(G\cdot C)$ Hoogsten triplet yielded an additional $\Delta\Delta G(25°C) = 5 \text{ kJ}\cdot\text{mol}^{-1}$ (22,23). Thus, the R-triplex stability estimated here at $\Delta\Delta G(0°C) = 1.8 \pm 0.2 \text{ kJ}\cdot\text{mol}^{-1}$ corresponds to the weakest hydrogen bonds observed in nucleic acid base pairs (24).

A relatively high contribution of hydrogen bonds to the R-triplex stability

Unlike the absolute average contribution of H-bonds to the overall DNA structures stability, the relative impact of hydrogen bonds in R-triplex differs significantly from those in duplex and conventional triplex DNA; i.e. the contribution of a single hydrogen bond to the R-triplex formation enthalpy $\Delta\Delta H/\Delta H = 18 \text{ kJ}\cdot\text{mol}^{-1}/99 \text{ kJ}\cdot\text{mol}^{-1} \approx 0.17$ is quite substantial (Table 1). The relative free energy contribution of an H-bond to the R-triplex stability is even greater,

$\Delta\Delta G(0°C)/\Delta G(0°C) = 1.8 \text{ kJ}\cdot\text{mol}^{-1}/7.1 \text{ kJ}\cdot\text{mol}^{-1} \approx 0.25$ (Table 1). In contrast, the relative impact of an additional hydrogen bond to the free energy as well as to formation enthalpy of the H-form triplex for an 11 nt long pyrimidine sequence is 0.09 (23). These values are close to the corresponding estimations for DNA duplexes (21,24,25).

The origin of this difference between the R-triplex and the H-triplex is the appreciably lower overall stability of the R-triplex, whose formation enthalpy is only $-10 \text{ kJ}\cdot\text{mol}^{-1}$ per base contact (Table 1 and Figure 5), whereas the average formation enthalpy for the H-triplex (26–28) and DNA duplex (29–31) are about $-30 \text{ kJ}\cdot\text{mol}^{-1}$. The low stability of the R-triplex is related to its structural features: (i) poor base stacking along the R-strand (5) and (ii) major 'sub-grooves' geometries, that may be less favorable for interactions with ions and water molecules compared with the H-triplex (32). At the same time, the R-triplex stability is extremely sensitive to the sequence, as stated previously.

CONCLUSIONS

(i) The formation of the R-triplex exclusive of an alternative 'branch migration' structure has been confirmed directly by strand-specific labeling using the fluorescence base analog 2-aminopurine (2AP).

(ii) Strand exchange could be promoted by substitution of two adenines in the third R-strand by 2,6-diaminopurine (DAP) due to a greater stability of the $DAP\cdot T$ base pair in comparison with the $A\cdot T$ base pair.

(iii) The hydrogen bonding scheme of the previously proposed (5) $A*(T\cdot A)$ R-type triplet was strongly supported by the results of adenine substitutions that

increased (2,6-diaminopurine) or decreased (7-deazaadenine) the number of hydrogen bonds in the fold.

(iv) The relative impact of hydrogen bonds on the overall stability of the R-triplex was significant (compared to the stability of a DNA duplex or an H-triplex).

(v) The large impact of a 'correct' base in the third strand opposite the Watson–Crick base pair on the thermodynamic properties of the R-triplex may be a powerful mechanism for ensuring proper recognition of the nucleic acid duplex by the single strand.

SUPPLEMENTARY DATA

Supplementary Data are available at NAR Online.

ACKNOWLEDGEMENTS

Conflict of interest statement. None declared.

REFERENCES

1. Howard-Flanders,P., West,S.C. and Stasiak,A. (1984) Role of RecA protein spiral filaments in genetic recombination. *Nature*, **309**, 215–219.
2. Griffith,J.D., Comeau,L., Rosenfield,S., Stansel,R.M., Bianchi,A., Moss,H. and de Lange,T. (1999) Mammalian telomeres end in a large duplex loop. *Cell*, **97**, 503–514.
3. Rocher,C., Letellier,T., Copeland,W.C. and Lestienne,P. (2002) Base composition at mtDNA boundaries suggests a DNA triple helix model for human mitochondrial DNA large-scale rearrangements. *Mol. Genet. Metab.*, **76**, 123–132.
4. Grewal,S.I. and Moazed,D. (2003) Heterochromatin and epigenetic control of gene expression. *Science*, **301**, 798–802.
5. Zhurkin,V.B., Raghunathan,G., Ulyanov,N.B., Camerini-Otero,R.D. and Jernigan,R.L. (1994) A parallel DNA triplex as a model for the intermediate in homologous recombination. *J. Mol. Biol.*, **239**, 181–200.
6. Van Meervelt,L., Vlieghe,D., Dautant,A., Gallois,B., Precigoux,G. and Kennard,O. (1995) High-resolution structure of a DNA helix forming (C.G)∗G base triplets. *Nature*, **374**, 742–744.
7. Spink,N., Nunn,C.M., Voitechovsky,J., Berman,H.M. and Neidle,S. (1995) Crystal structure of a DNA decamer showing a novel pseudo four-way helix–helix junction. *Proc. Natl Acad. Sci. USA*, **92**, 10767–10771.
8. Dagneaux,C., Liquier,J. and Taillandier,E. (1995) FTIR study of a nonclassical dT10∗dA10-dT10 intramolecular triple helix. *Biochemistry*, **34**, 14815–14818.
9. Dagneaux,C., Gousset,H., Shchyolkina,A.K., Ouali,M., Letellier,R., Liquier,J., Florentiev,V.L. and Taillandier,E. (1996) Parallel and antiparallel A∗A-T intramolecular triple helices. *Nucleic Acids Res.*, **24**, 4506–4512.
10. Shchyolkina,A.K., Timofeev,E.N., Borisova,O.F., Il'icheva,I.A., Minyat,E.E., Khomyakova,E.B. and Florentiev,V.L. (1994) The R-form of DNA does exist. *FEBS Lett.*, **339**, 113–118.
11. Shchyolkina,A.K., Borisova,O.F., Minyat,E.E., Timofeev,E.N., Il'icheva,I.A., Khomyakova,E.B. and Florentiev,V.L. (1995) Parallel purine–pyrimidine–purine triplex: experimental evidence for existence. *FEBS Lett.*, **367**, 81–84.
12. Shchyolkina,A.K., Timofeev,E.N., Lysov,Y.P., Florentiev,V.L., Jovin,T.M. and Arndt-Jovin,D.J. (2001) Protein-free parallel triple-stranded DNA complex formation. *Nucleic Acids Res.*, **29**, 986–995.
13. Shchyolkina,A.K., Kaluzhny,D.N., Borisova,O.F., Hawkins,M.E., Jernigan,R.L., Jovin,T.M., Arndt-Jovin,D.J. and Zhurkin,V.B. (2004) Formation of an intramolecular triple-stranded DNA structure monitored by fluorescence of 2-aminopurine or 6-methylisoxanthopterin. *Nucleic Acids Res.*, **32**, 432–440.
14. Xu,D., Evans,K.O. and Nordlund,T.M. (1994) Melting and premelting transitions of an oligomer measured by DNA base fluorescence and absorption. *Biochemistry*, **33**, 9592–9599.
15. Jean,J.M. and Hall,K.B. (2002) 2-Aminopurine electronic structure and fluorescence properties in DNA. *Biochemistry*, **41**, 13152–13161.
16. Cheong,C., Tinoco,I.,Jr and Chollet,A. (1988) Thermodynamic studies of base pairing involving 2,6-diaminopurine. *Nucleic Acids Res.*, **16**, 5115–5122.
17. Schyolkina,A.K., Kaluzhny,D.N., Borisova,O.F., Arndt-Jovin,D.J., Jovin,T.M. and Zhurkin,V.B. (2003) Formation of parallel recombination type triplex by human telomeric sequences. *J. Biomol. Struct. Dyn.*, **20**, 868–869.
18. Kim,M.G., Zhurkin,V.B., Jernigan,R.L. and Camerini-Otero,R.D. (1995) Probing the structure of a putative intermediate in homologous recombination: the third strand in the parallel DNA triplex is in contact with the major groove of the duplex. *J. Mol. Biol.*, **247**, 874–89.
19. Wahl,M.C. and Sundaralingam,M. (1997) C-H...O hydrogen bonding in biology. *Trends Biochem. Sci.*, **22**, 97–102.
20. Saenger,W. (1984) Principles of nucleic acid structure. In Cantor,C. R. (ed.), *Springer Advanced Texts in Chemistry*. Springer Verlag, NY, Berlin, Heidelberg, Tokyo.
21. Bloomfeld,V.A., Crothers,D.M. and Tinoco,I.,Jr (2000) *Nucleic Acids: Structures, Properties and Functions*. University Science Books, Sausalito, CA.
22. Frank-Kamenetskii,M.D. and Mirkin,S.M. (1995) Triplex DNA structures. *Annu. Rev. Biochem.*, **64**, 65–95.
23. Soliva,R., Guimil-Garcia,R., Blas,J.R., Eritja,R., Asensio,J.L., Gonzalez,C., Luque,F.J. and Orozco,M. (2000) DNA-triplex stabilizing properties of 8-aminoguanine. *Nucleic Acids Res.*, **28**, 4531–4539.
24. Turner,D.H., Sugimoto,N., Kierzek,R. and Dreiker,S.D. (1987) Free energy increment for hydrogen bonds in nucleic acid base pairs. *J. Am. Chem. Soc.*, **109**, 3783–3785.
25. Cubero,E., Guimil-Garcia,R., Luque,F.J., Eritja,R. and Orozco,M. (2001) The effect of amino groups on the stability of DNA duplexes and triplexes based on purines derived from inosine. *Nucleic Acids Res.*, **29**, 2522–2534.
26. James,P.L., Brown,T. and Fox,K.R. (2003) Thermodynamic and kinetic stability of intermolecular triple helices containing different proportions of C$^+$∗GC and T∗AT triplets. *Nucleic Acids Res.*, **31**, 5598–5606.
27. Soto,A.M. and Marky,L.A. (2002) Thermodynamic contributions for the incorporation of GTA triplets within canonical TAT/TAT and C$^+$GC/C$^+$GC base-triplet stacks of DNA triplexes. *Biochemistry*, **41**, 12475–12482.
28. Pilch,D.S., Levenson,C. and Shafer,R.H. (1991) Structure, stability, and thermodynamics of a short intermolecular purine–purine–pyrimidine triple helix. *Biochemistry*, **30**, 6081–6088.
29. Klump,H. and Ackermann,T. (1971) Experimental thermodynamics of the helix–random coil transition. IV. Influence of the base composition of DNA on the transition enthalpy. *Biopolymers*, **10**, 513–522.
30. Petruska,J., Goodman,M.F., Boosalis,M.S., Sowers,L.C., Cheong,C. and Tinoco,I.,Jr (1988) Comparison between DNA melting thermodynamics and DNA polymerase fidelity. *Proc. Natl Acad. Sci. USA*, **85**, 6252–6256.
31. SantaLucia,J.,Jr and Hicks,D. (2004) The thermodynamics of DNA structural motifs. *Annu. Rev. Biophys. Biomol. Struct.*, **33**, 415–440.
32. Malkov,V.A., Panyutin,I.G., Neumann,R.D., Zhurkin,V.B. and Camerini-Otero,R.D. (2000) Radioprobing of a RecA-three-stranded DNA complex with iodine 125: evidence for recognition of homology in the major groove of the target duplex. *J. Mol. Biol.*, **299**, 629–640.